Development of a test-bed technology for the Langmuir Probe investigation of dusty non-thermal plasmas

A. Woodard[1,2], K. Shojaei[2], C. Berrospe[2], G. Nava[2], and L. Mangolini[1,2]

[1] *Materials Science and Engineering Program, University of California Riverside, Riverside, California, USA*
[2] *Department of Mechanical Engineering, University of California Riverside, Riverside, California, USA*

Abstract: We present the development of a test-bed for the characterization of dusty plasmas via Langmuir probe. This diagnostic tool allows for the precise determination of the electron energy distribution function (EEDF) and subsequent plasma parameters/ but is notoriously difficult to use in dust-forming chemistries due to the formation of an insulating layer on the probe tip. In this work, we have designed a two-stage reactor scheme that overcomes the described limitation. In the first plasma reactor, the particle production cell, we synthesize graphitic carbon nanoparticles from the complete dissociation of acetylene. The nucleated particles are then seeded into the primary plasma where the Langmuir probe measurement is performed. The quality of the measurement is minimally affected by the presence of a graphitic nanoparticle coating on the probe tip due to its high electrical conductivity. Additionally, the approach has the advantage of decoupling the nucleation and growth-phase kinetics of the nanoparticles from the primary chamber discharge thus allowing us to study the effect of varying processing parameters on the dusty plasma properties. The trapping mechanism on the injected nanoparticles, induced by the primary plasma, was investigated to quantify the actual particle density in the reactor and the average charge per particle, through the measurement of continuous wave laser (532 nm) scattering intensity. The analysis of the EEDF as a function of the plasma parameters highlights the onset of unexpected trends in plasma the properties which are not predicted by theory.

Keywords: Langmuir probe, electron energy distributions, dusty plasma.

1. General

Low-temperature gas discharges are employed in a plethora of industrial fields, from thin-film deposition, material functionalization, and etching [1], to material synthesis [2,3]. The formation of dust is an overarching issue in plasma processing, and the initial discovery and subsequent investigation of particle-related phenomena in these discharges led to the foundation of dusty plasma science. While the formation of dust in such conditions was initially only seen as a detrimental side-product [4,5], that view later expanded to encompass dusty plasmas as a viable and controllable route for nanopowder fabrication. In order to advance these techniques and promote innovation, an increased knowledge of the fundamental physics and properties of dusty plasmas is not only desirable, but also a necessary step in understanding such systems, and thus a step towards engineering and optimization.

There are several experimental techniques for the characterization of plasmas [6]–[8]. The Langmuir probe, is one of the most established routes to obtain information on gas discharges; an in-depth analysis of the I-V characteristic provides information on the ion and electron densities, the electron temperature, and of course, the EEDF [9]. While this technique has been a driving force for most of the knowledge experimentally obtained regarding gas discharges, Langmuir probes are notoriously difficult to employ in dusty plasmas due to the insulating coating that accumulates at the probe tip preventing reliable measurements of EEDFs [10]. In this contribution we employ a non-conventional approach based on a two-stage reactor to overcome the above-mentioned limitations. In a first reactor, the nanoparticles generation cell, we produce highly-conductive graphitic carbon nanoparticles from the complete dissociation of C_2H_2 (acetylene) in a non-thermal plasma radiofrequency discharge. The particles are then seeded into the primary plasma where the Langmuir probe measurement is performed. By purposely using conductive nanoparticles, the formation of an insulating layer on the probe tip is prevented, allowing for reliable measurements in dust-rich conditions. Moreover, the described approach enables a simple strategy to study the influence of the variation of process parameters on the dusty plasma properties without affecting the nucleation and growth of the particles which is fully decoupled from the primary discharge in which the measurement is performed. In this contribution we compare the plasma properties of the primary discharge measured in dust-free and dust-rich conditions at fixed RF power.

2. Experimental

Fig. 1 depicts a schematic of the chamber setup. The nanoparticle production cell which produced and delivered the conductive carbonaceous particles was a capacitive discharge driven by an RF (80 W forward power). The gas mixture was comprised of 30 sccm Ar, 1.3 sccm H2, and 0.42 sccm C2H2, at a pressure of 1.5 Torr. A 2-mm orifice was used to maintain the pressure difference between the primary chamber and production cell.

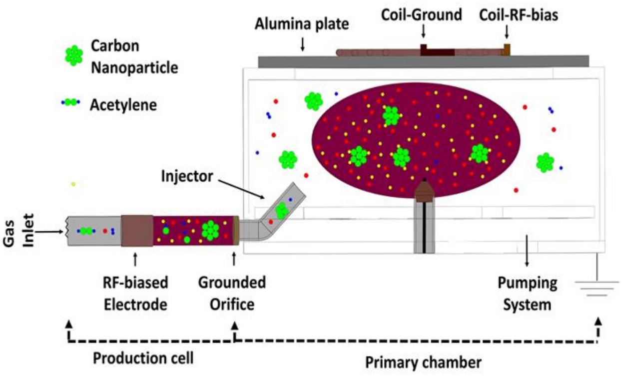

Fig 1. A schematic of the vacuum chamber showing the Langmuir probe and injection of carbon particles.

Particles were flown through a borosilicate tube for direct injection into the primary plasma volume. In the primary chamber, an Ar-H2 inductively coupled plasma is produced by delivering RF power to a three-turn planar coil. The measurements were performed in the bulk of the Ar-H2 plasma by a stationary Langmuir probe. The probe employs a self-compensating design to eliminate RF disturbances to the acquired signal [11,12]. The I-V characteristic of the probe was obtained by a PicoScopeTM and the subsequent software. A signal generator in conjunction with a high-voltage amplifier produced a linear ramp of –50 to +50 V at a frequency of 10 Hz as the probe voltage; the returning signal was fed through either a 30 or 330 **Ω** resistor. A differential amplifier was used to record the potential drop across the resistor and return the probe current waveform. The EEDF, F(E), and the electron energy probability function, f(E), were obtained from the I-V characteristic of the probe by following the Druyvesteyn method [13]. The electron, ne, and ion, nion, densities, electron temperature, Te, and the particle charge, Q, were obtained from F(E) following the procedure developed by Woodard et. al. [14]. By monitoring the deficit between ne, and nion densities the charge per particle can be obtained when the nanoparticle density np is known.

We have developed a model on the basis that in a self-sustaining steady state discharge plasma, electron-ion creation by ionization events needs to balance electron-ion loss due to recombination at the nanoparticle surfaces. Therefore, electron energy probability function is obtained self-consistently and iteratively considering quasi-neutrality condition and charge balance hold. Moreover, the numerically obtained EEPF is validated against the experimental findings. The trapping effect of nanoparticles, created in the plasma, was studied by recording the scattering intensity of a C.W laser (532 nm) focused inside of the primary chamber with an achromatic double lens (f= 400 mm), by a commercial camera. With the help of image processing tools, the scattered light was quantified as a function of time to calculate the particle density and the average charge per particle.

3. Results and Discussion

3.1 The setup working principle

Fig.2 displays the typical morphology of the graphitic carbon particles created in the production cell showing well-defined "graphene-like" fringes. Raman Spectroscopy, not shown here for brevity, was used to further confirm the high degree of graphitization of the produced material [14.]

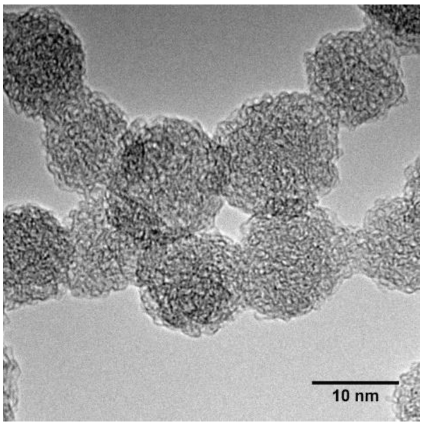

Fig 2. TEM image of the as-produced Carbon particles, with an average diameter of 14nm

The injection of carbon particle in the primary reactor produces, as expected, a coating on the Langmuir probe tip. Such coating however does not noticeably disturb the probe characteristics as a result of the high electrical conductivity of the synthesized carbon materials. A comparison among the *f(E)s* of a dust free Ar-H_2 plasma obtained before nanoparticle injection, after 12 min nanoparticles injection and after prolonged probe tip

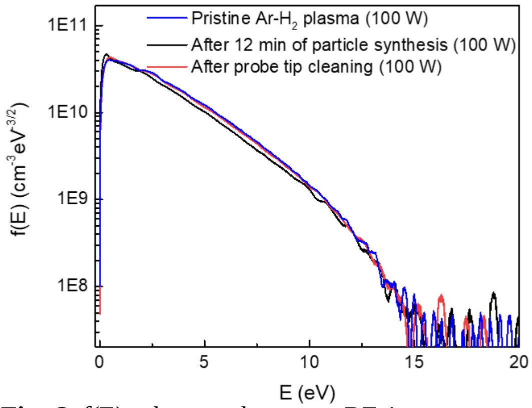

Fig. 3 *f(E)* taken at the same RF input power in the pristine, Ar-H_2 case, after an extended amount of nanoparticle flow to exaggerate the coating effect, and after electron bombardment to return the probe to a pristine state.

cleaning by ion bombardment is displayed in **Fig. 3** for reference. The *f(E)* is minimally affected by the prolonged particle deposition on the probe tip (the normal measurement time is three minutes).

3.2 The influence of particle injection on the primary plasma properties

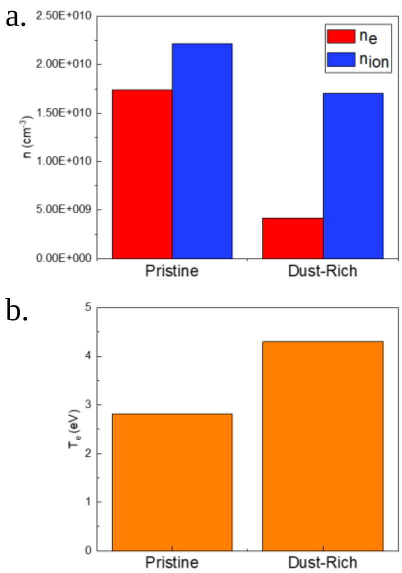

Fig. 4 (a) ne, nion and (b) Te for pristine and dust-rich plasma.

In a previous work, the measurement system presented in this contribution was used for studying the effect of the primary plasma power on in dust rich conditions at 150 mTorr [14]. We now focus our attention on the analysis of a plasma generated at lower pressure, i.e. 15 mTorr, and compare the dust-free and dust-rich condition. As expected from theory and previous literature, the injected nanoparticles act as electron sinks in the primary plasma and severely deplete the electron density, i.e. n_e decreases, while the electron temperature increases T_e (see **Fig. 4**) [14]. However, in the low-pressure condition employed in the described experiments, where the plasma density is sufficiently low, the particles induce an interesting effect that is not described by previous investigations. As seen in **Fig. 5**, a peak at 2.8 eV occurs in the EEDF.

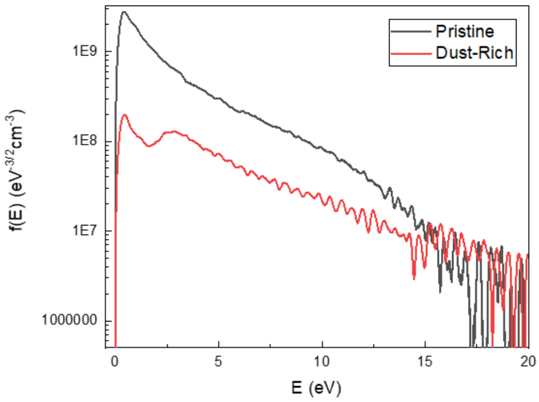

Fig. 5 f(E) for pristine and dust-rich plasma.

To understand the significance of this peak, we have performed simulations with a Boltzmann-solver. From **Fig. 6**, when the model is modified to account for the effect of secondary emissions, such as thermionic and secondary electron emission processes from the particles surface, a kink appears at the same energy.

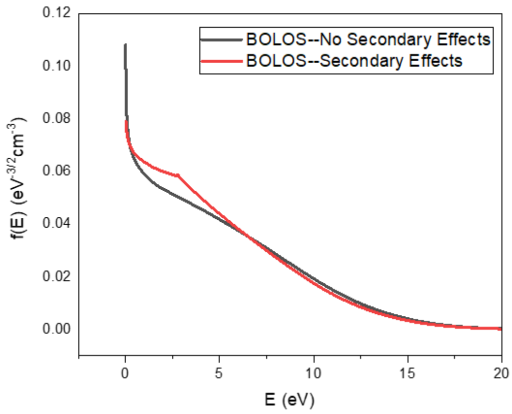

Hence, we cautiously attribute the observed phenomenon to this secondary emission processes, directly tied to the floating potential of the particle. Notably, while on the one hand the particles significantly alter the properties of the pristine plasma, on the other hand the presence of the discharge modifies significantly the dynamics of the particle in the primary chamber and prolong their residence time. This interesting trapping effect, which is attributed to charging of the particles and their permanence in a complex electromagnetic environment, was observed and quantified through a laser scattering experiment. The laser scattering of the carbon nanoparticles as a function of time is presented in Fig 7. The image sequence shows the increase of the scattered laser line intensity in time, therefore, indicating the increase of nanoparticle density trapped in the primary chamber. This is demonstrated in Figure 7b, where the average value of all the pixels designated to the laser line were plotted for each image (recorded every 30 seconds). The scattering intensity linearly increases in time, reaching a saturation point around 5 minutes. It is important to mention that plasma emission background was subtracted for every case. While the particle injection in the plasma can be measured with a simple gravimetric method, the described experimental evidence, shown also in **Fig. 7**, suggests that the actual particle density in the primary discharge is at least ten times higher than this value.

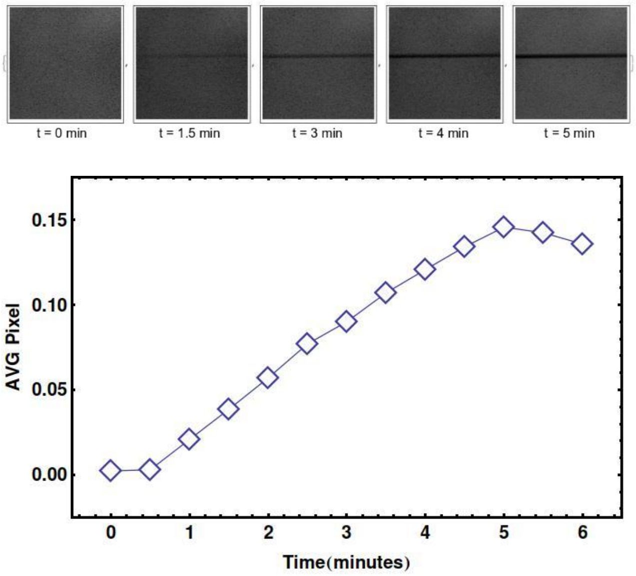

Fig. 7 (top) Image sequence of the scattered laser inside the primary plasma. (bottom) Pixel average of the laser line as a function of time for carbon nanoparticles produced at 0.42 sccm of C_2H_2.

4. Conclusions

We have developed test-bed to experimentally probe the effect of processing parameters on plasma properties in a dust-containing environment which surpasses the typical limitations characterizing previous attempts, most notably probe surface contamination and formation of insulating coatings. An Ar-H_2 non-thermal plasma controllably dosed with conductive graphitic nanoparticles has been used as an example. The true n_p in the discharge has been monitored with laser scattering and appears to be at least an order of magnitude larger than the mass injection rate would imply. We have preliminary results indicating that at the lower pressure condition (15 mTorr), a peak attributed to secondary electron effects at the nanoparticle surface emerges. A more comprehensive exploration of the processing parameters and the effect this has on the observed phenomena will be explained in detail.

References

[1] M. a Lieberman, *et al.*, *MRS Bull.*, vol. 30, no. November, pp. 899–901, 2005.

[2] L. Mangolini, *et al.*, *Nano Lett.*, vol. 5, no. 4, pp. 655–659, 2005.

[3] U. R. Kortshagen, *et al.*, *Chem. Rev.*, vol. 116, no. 18, pp. 11061–11127, 2016.

[4] Selwyn G.S., Heidenreich J.E., and Haller K.L. 1991, *Journal of Vacuum Science & Technology A.* **9**(5) 2817-2824.

[5] Selwyn G.S., Singh J., and Bennett R.S. 1989, *Journal of Vacuum Science & Technology A.* **7**(4) 2758-2765.

[6] N. Behlman, *J. Chem. Inf. Model.*, vol. 53, no. 9, pp. 1689–1699, 2013.

[7] T. Tsankov, *et al.*, *Plasma Process. Polym.*, vol. 3, no. 2, pp. 151–155, 2006.

[8] V. A. Godyak, *et al.*, *Plasma Sources Sci. Technol.*, vol. 11, no. 4, pp. 525–543, Nov. 2002.

[9] Godyak V.A., Piejak R.B., and Alexandrovich B.M. 1993, *Journal of Applied Physics*. **73**(8) 3657-3663.

[10] N. Bilik, *et al.*, *J. Phys. D. Appl. Phys.*, vol. 48, no. 10, p. 105204, 2015

[11] Chatterton P.A., Rees J.A., Wu W.L., and Al-Assadi K. 1991, *Vacuum*. **42**(7) 489-493.

[12] Sudit I.D. and Chen F.F. 1994, *Plasma Sources Science and Technology*. **3**(2) 162.

[13] Druyvesteyn M.J. 1930, *Zeitschrift für Physik*. **64**(11) 781-798.

[14] A. Woodard, *et al.*, *Plasma Sources Science and Technology*, vol. 27, no. 10.